Biomaterials Science

PAPER

View Article Online
View Journal

Cite this: DOI: 10.1039/c6bm00404k

In vitro detection of human breast cancer cells (SK-BR3) using herceptin-conjugated liquid crystal microdroplets as a sensing platform

Wang Ding,[a] Kailash Chandra Gupta,[a,c] Soo-Young Park,[a] Young-Kyoo Kim[b] and Inn-Kyu Kang*[a]

Received 15th June 2016,
Accepted 1st August 2016

DOI: 10.1039/c6bm00404k

www.rsc.org/biomaterialsscience

The present study utilizes antibody–protein interactions to develop an LC microdroplet based biosensor for naked eye detection of SK-BR3 human breast cancer cells. The herceptin antibody-conjugated LC microdroplets were fabricated using 4-cyano-4′-pentyl biphenyl (5CB) as the liquid crystalline phase and sodium dodecyl sulfate (SDS) as the surfactant. The poly (styrene-*b*-acrylic acid) amphiphilic block co-polymer (PS-*b*-PA) played a role as a modifier for the liquid crystalline interfaces. The 5CB molecules in the herceptin antibody-conjugated LC microdroplets have shown an orientation transition from radial to bipolar on selective interactions with targeted SK-BR3 breast cancer cells, which are over expressed by the human epidermal growth factor receptor 2-positive (HER2). The herceptin antibody-conjugated LC microdroplets are found to be highly selective in the detection of SK-BR3 cancer cells in the presence of control cells, such as KB cancer cells and fibroblast (FB), and also in the presence of 10% human blood plasma. The interaction forces of the SK-BR3 cancer cells were only effective in causing orientation transitions in 5CB molecules in the LC microdroplets, which clearly suggested that the herceptin antibody-conjugated LC microdroplets could be used as a selective biosensor for a real-time detection of SK-BR3 cancer cells in biological fluids.

1. Introduction

Liquid crystalline materials and technology have contributed significantly to the development of label-free, highly sensitive real-time detection devices without using complex and expensive instrumental paraphernalia. Liquid crystal (LC) surfaces and interfaces are potentially useful in sensing applications as their associated long range interfacial interaction forces are sufficiently high enough to extend deeply into the bulk liquid crystalline mesophase to create an optical signal. Liquid crystalline materials are very convenient for the fabrication of sensors for transduction of interfacial chemical/biological events into visible optical signals.[1,2] The long-range orientation ordering transitions and LC phase fluidity are triggered by the interactions of molecules at LC/water interfaces, which played a significant role in the fabrication of biosensors.[3,4] Surfactant anchored LC phase sensors have been developed for selective detection of cholic acid binding,[5] enzyme specific reactions,[6–9] protein adsorption,[10–13] environmental pollutants,[14,15] antigen–antibody immunoassaying,[1,16,17] DNA hybridization[18,19] and DNA oligonucleotides interactions.[20] With the increasing incidences of breast cancer amongst women, early detection and diagnosis has become a necessity to reduce the rate of mortality and to enhance the chances of patient survival.[21,22] In the absence of an effective sensing system, it has become difficult to diagnose breast cancer at an early stage. Though mammography has improved and is the clinical diagnosis for the detection of breast cancer, this technique is still inefficient and cannot detect 10–25% of tumors in women.[23,24] Significant progress has been made in tumor detecting markers, but predictive markers for breast cancer are still elusive. The commonly used breast cancer drugs, such as tamoxifen or raloxifene, are ineffective in curing the patients suffering from breast cancer in advanced stages.[25] In comparison to estrogen expressing (ER) breast cancers, the human epidermal growth factor receptor 2-positive (HER2) expressing breast cancers have shown the worst prognosis.[26] The anti-HER2 humanized recombinant monoclonal antibody (hercep-

[a]*Department of Polymer Science and Engineering, Kyungpook National University, 80, Daehak-ro, Buk-gu, Daegu 702-701, South Korea. E-mail: ikkang@knu.ac.kr, psy@knu.ac.kr, wangding0420@gmail.com; Fax: +82-53-950-6623; Tel: +82-53-950-5629*

[b]*Organic Electronic Laboratory, Department of Chemical Engineering, Kyungpook National University, 80, Daehak-ro, Buk-gu, Daegu 702-701, South Korea. E-mail: ykimm@knu.ac.kr*

[c]*Polymer Research Laboratory, Department of Chemistry, I.I.T. Roorkee, Roorkee 247667, India. E-mail: kcgptfcy@iitr.ac.in; Fax: +91 1332 273560; Tel: +91 1332 285325*

tin) has shown considerable clinical utility in inhibition of HER2 overexpression both in anti-metastatic[27,28] and adjuvant[29–31] chemotherapies, which significantly improved the prognosis of women with breast cancer. A double mastectomy is also another preventative measure amongst women with a high-risk of breast cancers. Numerous medical imaging methods, such as radionuclide imaging[32–35] and magnetic resonance imaging (MRI),[36] have been utilized for the detection of cancer. Radionuclide imaging is poor in spatial resolution and it requires radioactive compounds, which intrinsically have a limited half-life and expose the patient and practitioner to ionizing radiation. Early radionuclide imaging studies have demonstrated a high sensitivity in detection of palpable lesions but late stage radionuclide imaging has limited sensitivity for the detection of small lesions.[37–39] The routine magnetic resonance imaging (MRI) in the detection of breast cancer is also ineffective in the detection of cancers at an early stage. However, MRI detection has been improved using avidin–gadolinium complexes as contrast agents[40,41] for the detection of cancers efficiently in mice, but it is still ineffective for early detection and diagnosis of breast cancer in women. Therefore, the development of a sensor for early detection of breast cancer is of great significance. The monoclonal antibodies are cancer-targeting agents as the cancer cells are over expressed with cancer specific antigens. Among the latest tools in the detection of cancer, aptamers have gained an increasing importance in fighting cancers because of their high affinity and specificity for the antigens. However, thus far no aptamer based system has been effective for the detection of SK-BR3 cancer cells in comparison to the antibody based system[42–45] because of the problems with their cell internalization.[46–49] The liquid crystal-based biosensors are part of a recent sensing technology in which the LC acts as an efficient transducer for interfacial biomolecular interactions and biological events,[50,51] turning them into optical signals visible with the naked eye.[6] The liquid crystal-based biosensors have been used in the detection of chemicals[52–54] and interfacial reactions.[55,56] Our recent studies have indicated that liquid crystalline molecules confined in a microdroplet are more sensitive in showing orientation transitions[57] in comparison to the stratified layered structures of LC on planner solid surfaces.[58,59] So far no study is available on the detection of SK-BR3 cells using herceptin antibody-conjugated LC sensors; hence, the present study has been carried out to develop an antibody-conjugated LC-microdroplets biosensor for early detection of SK-BR3 breast cancer cells in biological fluid. The antibody-conjugated LC microdroplets are more efficient in forming optical signals *via* interactions with cancer cells without using additional devices for signal transduction. The 5CB molecules at the LC microdroplets interface after interactions with the SK-BR3 cancer cells were able to induce orientation transitions throughout the bulk phase of the LC microdroplets. The orientation transitions in the 5CB molecules in LC microdroplets upon interactions with SK-BR3 cancer cells have produced naked eye detectable, real time signals, which have been monitored using a crossed-polarizing system. The major goal of the present study has been to develop herceptin antibody-conjugated LC microdroplets for *in vitro* targeted and sensitive detection of SK-BR3 cancer cells in simulated biological fluids in the presence of KB cancer cells and other cell lines for early diagnosis. This can lead to effective therapies for patients suffering from SK-BR3 human breast cancers.

2. Experimental section

2.1 Materials and chemicals

The nematic liquid crystal, 4-cyano-4′-pentyl biphenyl (5CB) (MW, 249.15 g mol^{-1}, m.p. 24 °C) was purchased from Tokyo Chemical Company Ltd Japan and used without further purification. Poly(styrene-*b*-acrylic acid) (PS-*b*-PA) (MW, 8×10^3 g mol^{-1}, PS: PA 0.6 : 1.0, PDI ≤ 1.1) was received from Sigma-Aldrich Chemical Company, USA. The *N*-(3-dimethylaminopropyl)-*N*′-ethylcarbodiimide (EDC), *N*-hydroxysuccinimide (NHS), sodium dodecyl sulfate (SDS) (MW, 288.38 g mol^{-1}), rhodamine 6G (MW, 479 g mol^{-1}), and methylene blue (MW, 319.85 g mol^{-1}) were purchased from Sigma-Aldrich Chemical Company, USA, and used as received without further purification. Plasma from humans was purchased from Sigma-Aldrich Chemical Company. Herceptin antibody (MW, 145.5×10^3 g mol^{-1}) was obtained from Roche Pharma Ltd, Basel, Switzerland. Cell culturing reagents, RPMI-1640 medium (RPMI-1640), Eagle's minimum essential medium (EMEM), Dulbecco's modified eagle medium (DMEM), fetal bovine serum (FBS), penicillin streptomycin G sodium (PGS) (50 units per mL and 50 mg mL^{-1}, respectively), TrypLETM Express (0.25% trypsin, 0.02% EDTA, TE) and Dulbecco's phosphate buffered saline (DPBS, pH 7.4) were purchased from Gibco, USA. The dialysis cellulose membranes (size: 43 mm × 27 mm, MWCO: 12 264) were purchased from Sigma-Aldrich, Chemical Company, USA. The SK-BR3 cancer cells (human breast cancer cells) and KB cells (epithelial cancer cells) were procured from American Type Culture Collection (ATCC), Manassas, VA, USA. FB cells (fibroblast cells) were procured from a cells bank in South Korea.

2.2 Formation of 5CB LC microdroplets

The O/W system was used to form LC microdroplets emulsion. In previous studies, the surfactant was used to control the stability of the LC microdroplets by preventing the coalescence of LC microdroplets[1,60–62] and controlling the interfacial tension of the LC microdroplets emulsion. However, in our studies, the PS-*b*-PA block copolymer played the role of surfactant because of its amphiphilic nature.[63] To prepare the LC microdroplets emulsion, 10 mg (2.50×10^{-3} mmol) of PS-*b*-PA was dispersed in a 10 mL solution of DPBS in a 30 mL stoppered conical flask. To this solution, 50 mg (0.173 mmol) of SDS was added under constant stirring at 500 rpm for about 1 h. After proper mixing of the PS-*b*-PA block copolymer and SDS surfactant, the LC microdroplets emulsion was prepared by drop-wise addition of 50 mg (0.2 mmol) of 5CB molecules to this mixture, and the resultant mixture was allowed to stir

vigorously for about 10 minute using a high speed homogenizer at 19 000 rpm to obtain monodispersed micrometer sized LC microdroplets. The resultant LC microdroplets emulsion was allowed to equilibrate for about 30 min, and then, the supernatant liquid containing extremely small sized LC microdroplets, unused SDS and PS-*b*-PA block copolymers was separated. The separated LC microdroplets were rinsed twice with fresh DPBS solution and finally stored in a DPBS solution for experimental work.

2.3 Conjugation of herceptin antibody with 5CB LC microdroplets

After fabrication of the 5CB LC microdroplets, the binding of herceptin was carried out using activated herceptin. To anchor the herceptin on the LC microdroplets, the carboxyl groups of the polyacrylic acid segments (PA) of the PS-*b*-PA block copolymer in the LC microdroplets were activated by adding EDC (0.4 M) and NHS (0.1 M) solutions and allowing them to react for about 1 h. The activated 5CB LC microdroplets then dispersed in a 10 mL DPBS buffer solution containing 500 μg herceptin and allowed to incubate for about 12 h at room temperature to obtain herceptin-anchored LC microdroplets. The herceptin antibody-anchored LC microdroplets were then rinsed with a PBS buffer solution (pH, 8.0) to remove any unused free herceptin. Finally, herceptin-anchored LC microdroplets were stored in a DPBS buffer solution for cell culturing experiments.

2.4 Size measurement and fluorescent imaging of 5CB LC microdroplets

To evaluate the size of the LC microdroplets and orientation of the 5CB molecules in the LC microdroplets before and after conjugation of herceptin, 1.0 mL of the LC microdroplets emulsion was placed in a dish 1.0 cm in diameter with the DPBS solution, and then, bright field and polarized optical microscopic (POM) images were recorded using a polarized optical microscope (Leitz, ANA-006, Germany) attached to a CCD camera (Samwon, STC-TC83USB, Korea). The charge density on the LC microdroplets was measured using zeta-potential (Zetasizer Nano ZS90, Malvern Instruments Ltd UK). To confirm the binding of herceptin on the polyacrylic acid segment of the PS-*b*-PA in the LC microdroplets, the herceptin–rhodamine-6G conjugate was also used to anchor on the LC microdroplets. The labeling of herceptin with rhodamine 6G was carried out by modifying the method as reported by Khan *et al.*[4] Briefly, 1.0 mg mL^{-1} solution of herceptin was prepared in a DPBS buffer solution (pH, 7.4), and the carboxyl groups of herceptin were activated by reacting EDC (0.4 M) and NHS (0.1 M) solutions at 0 °C for about 1 h. To this solution, 1.0 mg of rhodamine 6G was added, and the solution was stirred for about 12 h in the dark at room temperature. To stop the reaction, a saturated aqueous solution of ammonium sulfate (0.5 g mL^{-1}) was added, and the mixture was allowed to incubate for about 2 h at a low temperature. The resultant herceptin–rhodamine-6G conjugate was purified using a cellulose membrane (MWCO, 12 264) until the dialyzing fluid (DPBS) was clear. Finally, the herceptin–rhodamine-6G conjugate was stored in the dark in a quartz cuvette at 4 °C. Subsequently, the prepared herceptin–rhodamine-6G conjugate was anchored on the 5CB LC microdroplets following the procedure applied for binding the herceptin to the 5CB LC microdroplets. To remove the unused amount of herceptin–rhodamine-6G conjugate, the herceptin–rhodamine-6G conjugated LC microdroplets were washed with the DPBS buffer solution. To confirm the anchoring of the herceptin–rhodamine-6G conjugate on the LC microdroplets, the fluorescence images of the herceptin–rhodamine-6G conjugated LC microdroplets were captured using a fluorescence microscope (Olympus BX61) equipped with a fluorescent filter cube turret above the objective lenses and a digital camera. The fluorescence imaging of the LC microdroplets was carried out in triplicate at three different locations of the optical cell to get an average view of the LC microdroplets.

2.5 Cell culture

The cell culture base media for the SK-BR3 cancer cell line (RPMI-1640), KB cancer cell line (EMEM) and FB cell line (DMEM) were procured from Thermo Fisher Gibco. These cells were cultured at 37 °C in an incubator containing 5% CO_2 using a 10 mL base medium supplemented with 10% FBS and 1% PGS. The cell medium was changed every two days. In the sub-culturing experiments, the cells were washed twice with a DPBS buffer solution and after culturing, the cells were harvested using a TE solution for 4.0 min at 37 °C. The harvested cells were washed twice with a DPBS buffer solution and re-dispersed in complete media after centrifugation for reseeding and growth in fresh culture dishes. The morphology of the 3 day cultured cells was recorded at a cell density of 5×10^4 cells per mL in a 10 mL petri dish using an optical microscope (Nikon Eclipse TS100, Japan).

2.6 *In vitro* cells sensing using herceptin-conjugated 5CB LC microdroplets

In vitro cell interactions with LC microdroplets emulsion were evaluated by culturing selected cells with herceptin anchored 5CB LC microdroplets emulsion. In the present study, the SK-BR3 cancer cells, KB cancer cells and FB cells were cultured in polystyrene dishes in the presence of seeding media. After culturing the cells for 3 days, the cells were harvested using a TE solution and centrifuged at 800 rpm for 4 min. The harvested cells were rinsed with sterile DPBS media (pH, 7.4) containing calcium chloride (10 mM) and magnesium chloride (5 mM). These cells were re-dispersed in DPBS media (pH, 7.4) and the cell density was measured using a hemocytometer. To maintain a fixed density of cells (5000 cells per mL) in a culture dish containing the LC microdroplets emulsion, a calculated volume of medium of known cell density was added to the dish containing the herceptin-conjugated LC microdroplets to maintain a final cell density of 5000 cells per mL. This was incubated in the presence of a 10% human blood plasma solution for a contact time of 3 h at 30 °C in the presence of 5% CO_2. To confirm the interactions of the herceptin-anchored

LC microdroplets with the SK-BR3 cancer cells, KB cancer cells and FB cells, the bright field and POM micrographs were recorded after incubation for a period of 3 h. To analyze the selectivity of the herceptin-conjugated LC microdroplets for the detection of SK-BR3 cancer cells in the presence of KB cancer cells and FB cells, a calculated volume of SK-BR3, KB and FB cell medium of known cell density was used, and the density of each cell line was maintained at 2000 cells per mL in a culture dish containing the herpectin-conjugated LC microdroplets emulsion. To differentiate the interactions of the KB cancer cells, FB cells and SK-BR3 cancer cells with the LC microdroplets, the 10% methylene blue stained SK-BR3 cancer cells were incubated along with the herceptin-conjugated LC microdroplets. The KB cancer cells, FB cells and SK-BR3 cancer cells were incubated for 3 h in presence of 5% CO_2 at 30 °C with the herpectin-conjugated LC microdroplets in the presence of 10% human blood plasma. All the solutions were prepared in triple distilled water for experimental work. The optical and polarized light microscopic images of the LC microdroplets were recorded using a polarized optical microscope (Leitz, ANA-006, Germany) attached to a CCD camera (Samwon, STC-TC83USB, Korea).

3. Results and discussion

This study reports on the development of an antibody-conjugated LC microdroplets biosensor for the detection of SK-BR3 cancer cells rather than using stratified layered structures of LC molecules on solid surfaces.[62] In comparison to the solid surface based LC biosensors, the microdroplets confined LC biosensors are more efficient in transmitting the antibody–protein binding interactions throughout the LC microdroplets and in forming optical signals without using additional devices. In these studies, the 4-cyano-4′-pentyl-biphenyl (5CB, nematic liquid crystal) based microdroplets emulsion was prepared using an O/W emulsion system. The PS-*b*-PA block copolymer was used to stabilize the 5CB LC microdroplets emulsion because of its amphiphilic nature. The hydrophobic styrene block of the amphiphilic PS-*b*-PA block copolymer was assumed to be miscible with the hydrophobic parts of the 5CB molecules, which formed an inner core of LC microdroplets. Whereas, the hydrophilic polyacrylic acid block of the amphiphilic PS-*b*-PA block copolymer formed an outer shell around the LC microdroplets.[63] The herceptin antibody is conjugated with the polyacrylic acid segment of the amphiphilic PS-*b*-PA block copolymer to target the SK-BR3 cancer cells through HER2 receptors overexpressed on SK-BR3 cancer cell membranes. In the PS-*b*-PA block copolymer based LC microdroplets system, the polystyrene segments of the PS-*b*-PA block copolymer interacted strongly with the 5CB molecules in the LC microdroplets through permeation; whereas, the hydrophilic polyacrylic acid segments of the PS-*b*-PA block copolymer remained free at the surface of the LC microdroplets to control the interfacial tension of the LC microdroplets and to prevent the coalescence of LC microdroplets through electrostatic interactions.[63]

The herceptin-conjugated LC microdroplets upon interaction with the SK-BR3 cancer cells have shown orientation transitions in the 5CB molecules from radial to bipolar due to the antigen–antibodies interactions (Scheme 1).[57]

The bare 5CB LC microdroplets dispersed in an aqueous medium are stable in bipolar orientations,[62–65] but the observed radial orientation of the 5CB molecules in the prepared LC microdroplets (Scheme 1) is assumed to be due to the adsorption of the hydrophobic tail of the surfactant on the 5CB molecules. However, the hydrophilic head of the surfactant remained free at the interface of the LC microdroplets and did not influence the orientation of the 5CB molecules in the microdroplets.[66,67]

3.1 Optical and polarized light micrographs of LC microdroplets with and without herceptin antibody

To confirm the orientation of the 5CB molecules in the LC microdroplets and herceptin conjugated LC microdroplets, the optical and polarized light images were recorded, as shown in Fig. 1. The optical (top) and polarized (bottom) images of the LC microdroplets with 5CB molecules encapsulated with SDS and the PS-*b*-PA block copolymer confirmed the radial orientation of the 5CB molecules in the LC microdroplets (Fig. 1a and c).

This was assumed to be due to the permeation of the hydrophobic part of the SDS molecule through a layer of the PS-*b*-PA block copolymer and its interactions with the 5CB molecules in the LC microdroplets. Thus, the presence of SDS played a significant role in controlling the orientation of the 5CB molecules in the LC microdroplets.[66,67] The optical (top) and polarized (bottom) images of the LC microdroplets with 5CB molecules encapsulated with SDS and herceptin-conjugated PS-*b*-PA block copolymer are shown in Fig. 1b and d. These LC microdroplets also show 5CB molecules in a radial orientation, even after conjugating the herceptin antibody on the activated carboxylic groups of the PS-*b*-PA block copolymer.

This result suggested that the chemical binding of herceptin on the PS-*b*-PA block copolymer did not influence the radial orientation of the 5CB molecules in the LC microdroplets. The decreasing trend in the zeta potential of the 5CB LC microdroplets from −75.8 mV to −89.8 mV upon conjugation of the PS-*b*-PA block copolymer with the LC microdroplets and increasing trend in the zeta potential to −36.7 mV after conjugation of herceptin on the LC microdroplets confirmed the formation of layers of the PS-*b*-PA block copolymer and anchoring of herceptin with the PS-*b*-PA block copolymer on the 5CB molecules in the LC microdroplets. The polyacrylic acid block of the PS-*b*-PA copolymer has been considered to be responsible for the decrease in the zeta potential from −75.8 mV to −89.8 mV; whereas, the binding of herceptin increased the zeta potential to −36.7 mV. To further confirm the binding of herceptin with the polyacrylic acid segment of the PS-*b*-PA block copolymer in the LC microdroplets, the herceptin–rhodamine-6G conjugate was used to conjugate on

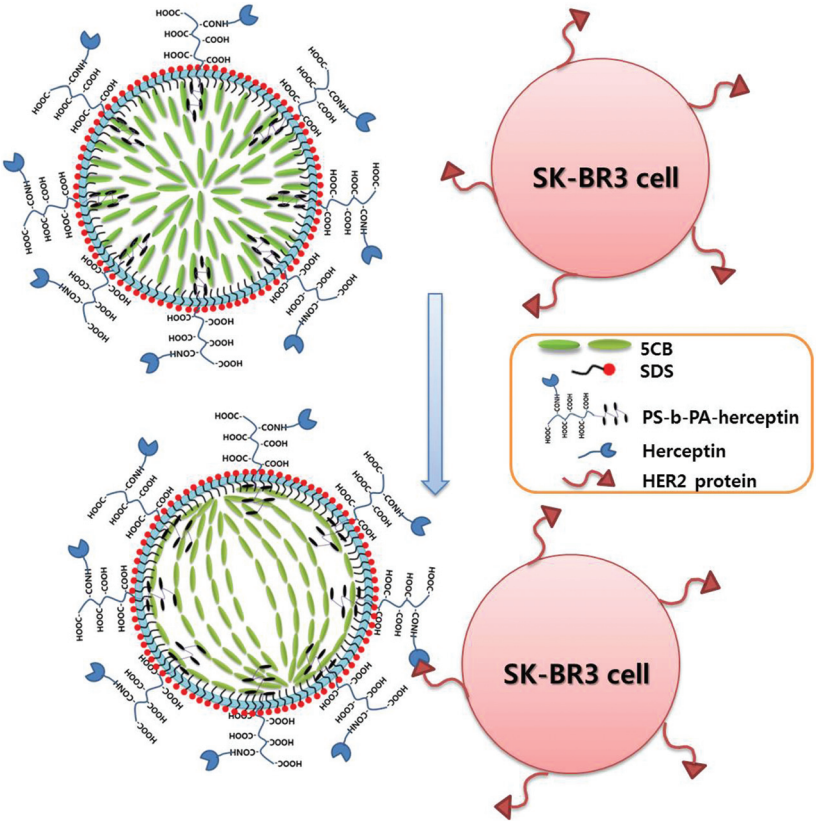

Scheme 1 Schematic illustration showing herceptin-HER2 interaction induced configuration transitions in LC microdroplets.

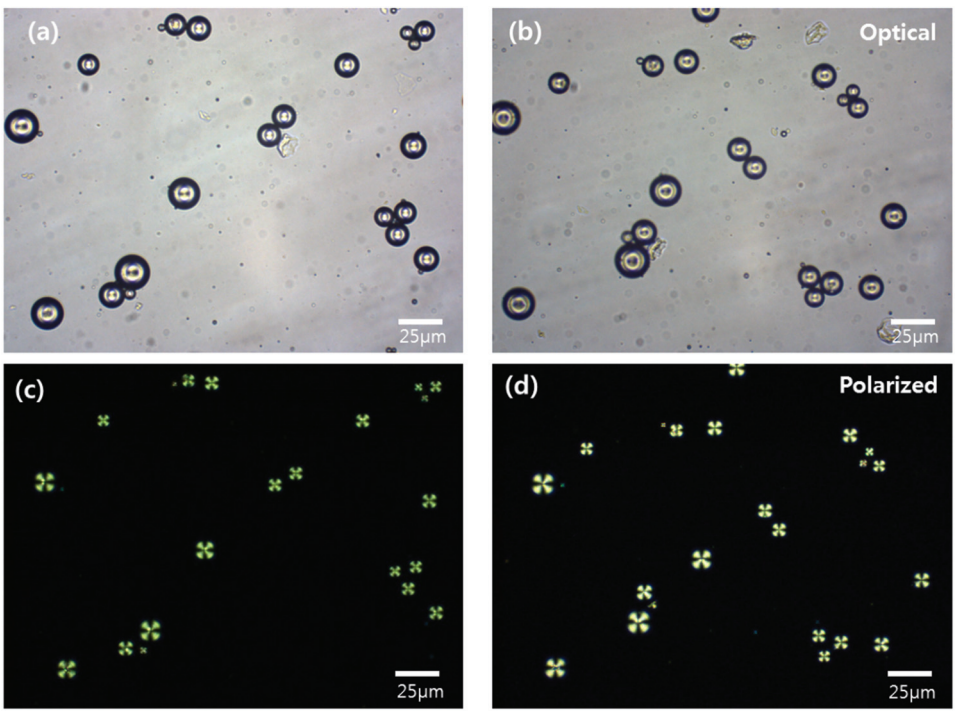

Fig. 1 Optical (top) and polarized light (bottom) images showing the configuration of the 5CB molecules in the LC microdroplets (a, c), and herceptin conjugated LC microdroplets (b, d).

the LC microdroplets following the procedure used for binding herceptin on the 5CB LC microdroplets. The resultant herceptin–rhodamine-6G conjugated microdroplets were used to record their fluorescence micrographs using a fluorescence microscope coupled with a digital camera, as shown in Fig. 2a. To record their optical and polarized light micrographs, the CCD camera (Samwon, STC-TC83USB, Korea) attached to a polarized optical microscope (Leitz, ANA-006, Germany) was used (Fig. 2b and c). The LC microdroplets were clearly visible as green spheres in the fluorescence image of herceptin–rhodamine-6G conjugated LC microdroplets (Fig. 2a).

The background of the optical images of the LC microdroplets suggests that herceptin was successfully anchored on the polyacrylic acid segments of the PS-*b*-PA block copolymer in the LC microdroplets. The herceptin–rhodamine-6G conjugated LC microdroplets retained the radial configuration of the 5CB molecules after anchoring of the herceptin–rhodamine-6G conjugate, as confirmed by the polarised light micrographs (Fig. 2c). The anchoring of the herceptin–rhodamine-6G conjugate on the 5CB LC microdroplets is further confirmed by recording a UV-Vis spectrum of the herceptin–rhodamine-6G conjugated LC microdroplets (Fig. 3a) and by comparing the spectrum with the UV-Vis spectra of pure rhodamine 6G (Fig. 3b) and herceptin (Fig. 3c). The presence of rhodamine 6G in herceptin–rhodamine-6G conjugated LC microdroplets is confirmed due to appearance of strong absorption band at 527 nm (Fig. 3a), which was present in UV spectrum of pure rhodamine 6G (Fig. 3b). The blue shift in the characteristic peak of herceptin from 228 to 207 nm also helped confirm its anchoring at the PS-*b*-PA block copolymer

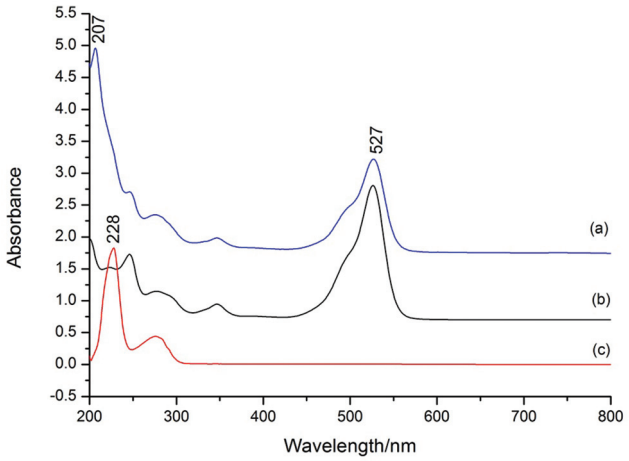

Fig. 3 UV–Vis spectra of herceptin–rhodamine-6G conjugated LC microdroplets (a), rhodamine 6G (b), and herceptin (c).

by forming an amide bond between the carboxylic acid of the polyacrylic acid segment of the PS-*b*-PA block copolymer and amino group of the herceptin.

These data confirmed the labeling of herceptin on the PS-*b*-PA block copolymer in the LC microdroplets. To evaluate the effect of the binding amount of herceptin on the orientation of the 5CB molecules in the LC microdroplets, the LC microdroplets were also loaded with different amounts of herceptin using herceptin–rhodamine-6G conjugate solutions of different concentrations (1, 10, 20, 50 μg mL^{-1}). The binding amount of the herceptin–rhodamine-6G conjugate on the

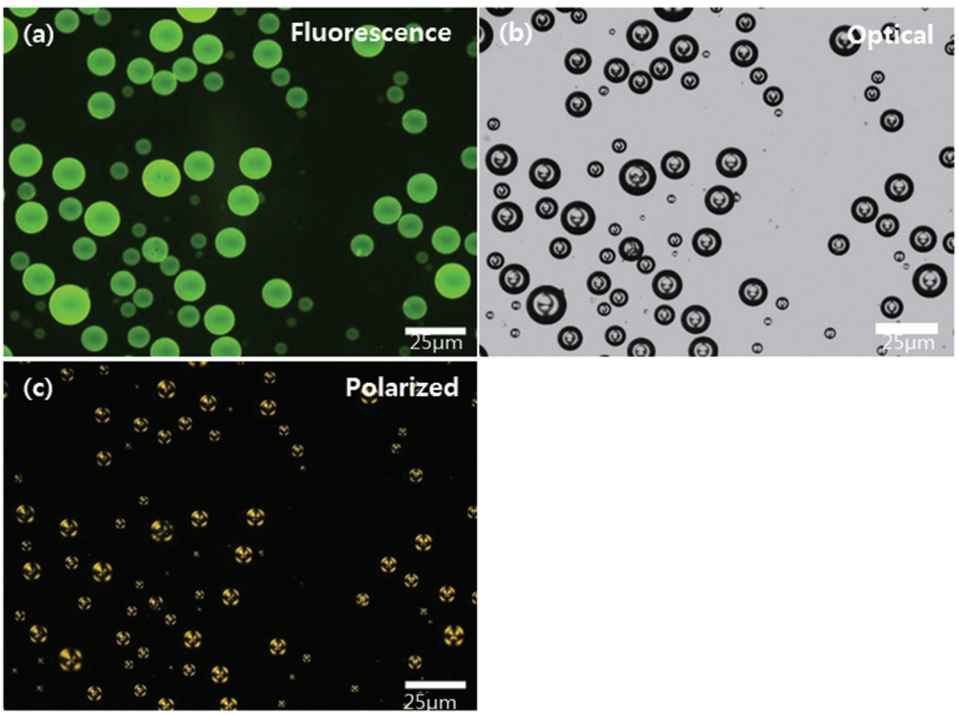

Fig. 2 Fluorescence (a), optical (b) and polarized light (c) images of herceptin–rhodamine-6G conjugated LC microdroplets.

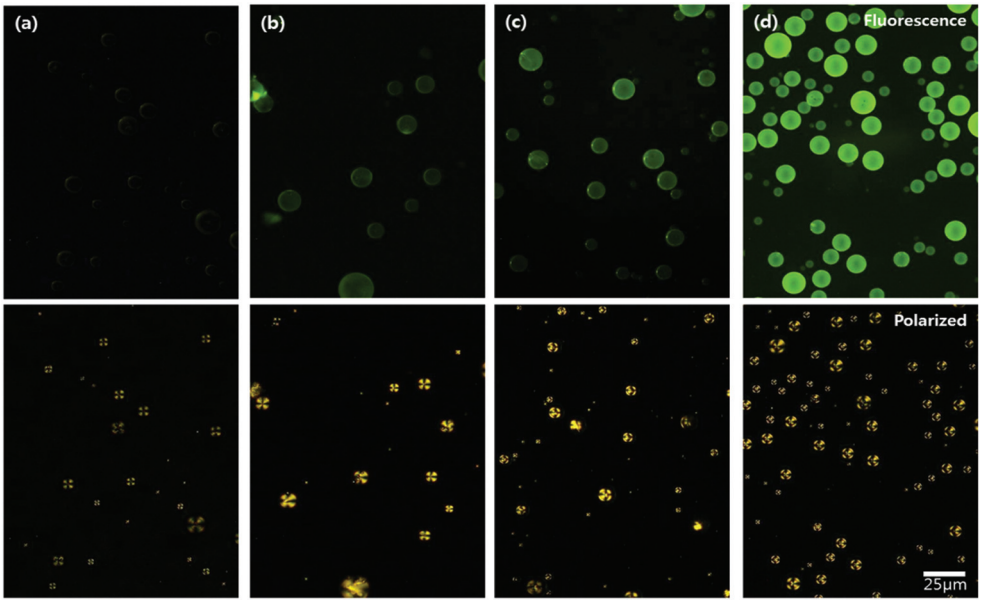

Fig. 4 Fluorescence (top) and polarized light (bottom) images of the 5CB LC microdroplets anchored with different amounts of herceptin using herceptin–rhodamine-6G conjugate solutions of different concentrations, 1 μg mL^{-1} (a), 10 μg mL^{-1} (b), 20 μg mL^{-1} (c) and 50 μg mL^{-1} (d).

LC microdroplets increased upon increasing the concentration of the herceptin–rhodamine-6G conjugate but no variation in the orientation state of the 5CB molecules in the LC microdroplets was observed. Upon loading a higher amount of the herceptin–rhodamine-6G conjugate, the LC microdroplets appeared to be brighter and deep green in color, as shown in the fluorescence images of the LC microdroplets (Fig. 4).

This result also suggested that more herceptin can be conjugated on the LC microdroplets using a concentrated solution of herceptin without altering the orientation of the 5CB molecules in the LC microdroplets. The LC microdroplets retained the radial configuration of the 5CB molecules irrespective of the loaded amount of herceptin, which suggested that the interaction forces of the conjugated herceptin were too weak to bring any configuration transition to the 5CB molecules in the LC microdroplets.

3.2 Optical response of herceptin-conjugated LC microdroplets for studied cells

To evaluate the sensing response of the herceptin-conjugated LC microdroplets on interactions with the SK-BR3 cancer cells, 1.0 mL of the herceptin conjugated LC microdroplets emulsion was cultured with SK-BR3 cancer cells, KB cancer cells and FB cells in 10% human blood plasma for 3 h at 30 °C with a cells density of 5000 cells per mL. The bright field and polarized light (crossed polar) images of the herceptin-conjugated LC microdroplets were recorded, as shown in Fig. 5, along with the director profile of the 5CB molecules in the LC microdroplets. The bright field images of the herceptin-conjugated LC microdroplets in the presence of SK-BR3 cancer cells, KB cancer cells and FB cells (Fig. 5a, c and e) confirmed the interactions of the herceptin-conjugated LC microdroplets with KB cancer cells (Fig. 5c), FB cells (Fig. 5e) and SK-BR3 cancer cells (Fig. 5a) as marked by the red circles. To evaluate the effect of cell interactions on the orientation state of the 5CB molecules in the LC microdroplets, the polarized light micrographs (POM) of herceptin-conjugated LC microdroplets were examined for SK-BR3 cancer cells, KB cancer cells and FB cells (Fig. 5b, d and f). The POM images of the herceptin-conjugated LC microdroplets recorded in the presence of SK-BR3 cancer cells indicated a change in orientation in the 5CB molecules in the LC microdroplets from radial to bipolar (Fig. 5b). However, the interactions of the KB cancer cells and FB cells with herceptin-conjugated LC microdroplets did not influence an orientation transition in the 5CB molecules from radial to bipolar (Fig. 5d and f).

These results clearly indicated that the interactions of the SK-BR3 cancer cells with herceptin-conjugated LC microdroplets were effective and selective to show an orientation transition from radial to bipolar in the 5CB molecules in the LC microdroplets (Fig. 5a and b); whereas, KB cancer cell (Fig. 5c and d) and FB cell (Fig. 5e and f) interactions were found to be ineffective. Hence, herceptin-conjugated 5CB LC microdroplets can be used for the selective detection of SK-BR3 cancer cells in biological fluids.

3.4 Effect of cell membrane morphology on the optical response of herceptin-conjugated LC microdroplets

To evaluate the effect of cellular morphology on the optical response of herceptin conjugated LC microdroplets, SK-BR3 cancer cells, KB cancer cells and FB cells were cultured in their media for a long time until the cell's membranes were spread completely, and these cells were cultured with 1.0 mL of the herceptin-conjugated LC microdroplets emulsion for 3 h at

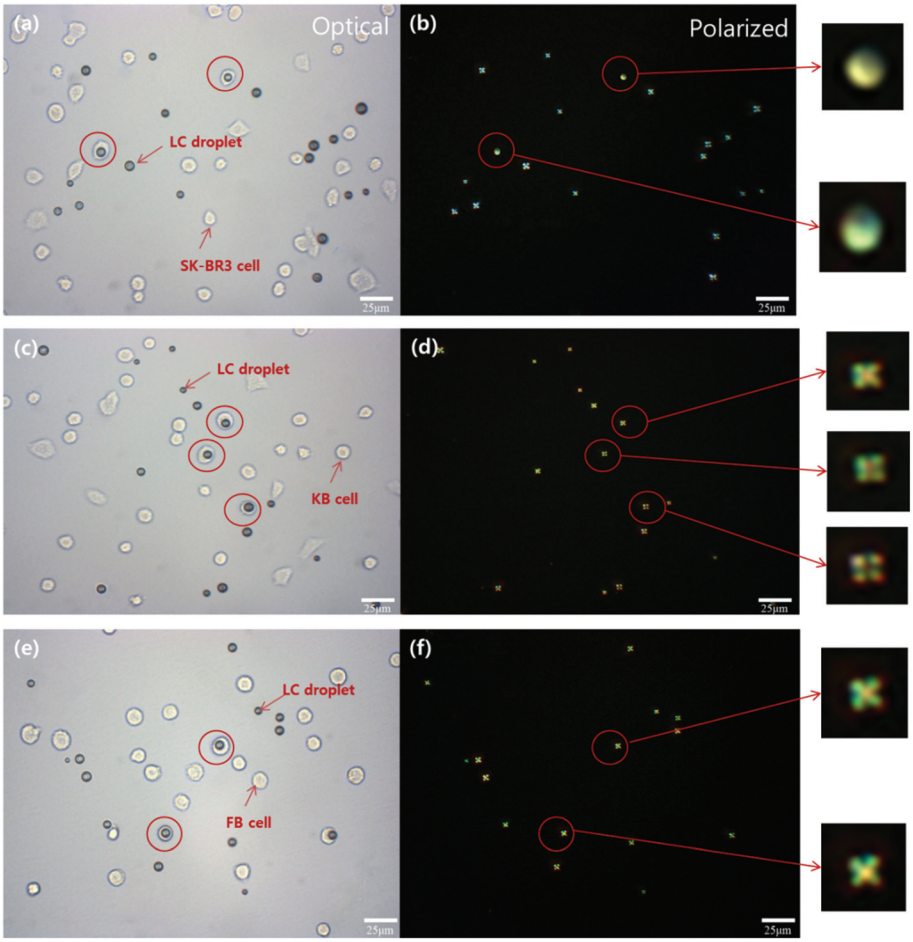

Fig. 5 Optical (left) and polarized light (right) images of herceptin-conjugated LC microdroplets showing interactions with the SK-BR3 cancer cells (a, b), KB cancer cells (c, d) and FB cells (e, f) in 10% human blood plasma.

30 °C with a cells density of 5000 cells per mL in 10% human blood plasma. To evaluate the effect of the cell membrane morphologies on the optical response of the herceptin-conjugated LC microdroplets, the bright field and polarized light (crossed polar) images of the herceptin-conjugated LC microdroplets were recorded, as shown in Fig. 6, along with the director profile of the 5CB molecules in the LC microdroplets. The bright field images of the SK-BR3 cancer cells, KB cancer cells and FB cells (Fig. 6a, c and e) have confirmed the interactions of the herceptin-conjugated LC microdroplets with SK-BR3 cells (Fig. 6a), KB cancer cells (Fig. 6c), FB cells (Fig. 6e), as indicated by the red marked circles.

To evaluate the effect of the cell membrane morphology on the orientation of the 5CB molecules in the LC microdroplets, the polarized light micrographs (Fig. 6b, d and f) of herceptin-conjugated LC microdroplets interacting with SK-BR3 cancer cells, KB cancer cells and FB cells were examined. The polarized light images of herceptin-conjugated LC microdroplets interacting with SK-BR3 cancer cells (Fig. 6b) indicated an orientation transition from radial to bipolar in the 5CB molecules. However, no orientation transition in the 5CB molecules in the herceptin-conjugated LC microdroplets was observed upon interacting with KB cancer cells (Fig. 6d) and FB cells (Fig. 6f).

These studies clearly indicated that the variation in the cell membrane morphologies of the SK-BR3 cancer cells, KB cancer cells and FB cells was ineffective in varying the responses of the herceptin-conjugated LC microdroplets, and the orientation states of 5CB molecules remained the same as those observed with fresh SK-BR3 cancer cells, KB cancer cells and FB cells (Fig. 5). These results indicated that the orientation transitions in the 5CB molecules in the herceptin-conjugated LC microdroplets remained selective to SK-BR3 cancer cells (Fig. 6a and b), which provides a strong basis to use herceptin-conjugated LC microdroplets for selective detection of SK-BR3 cancer cells in biological fluids.

3.5 Selectivity of herceptin-conjugated LC microdroplets for SK-BR3 cancer cells

To evaluate the selectivity of the herceptin-conjugated LC microdroplets for detection of SK-BR3 cancer cells, the detection of SK-BR3 cancer cells by herceptin-conjugated LC microdroplets was carried out in the presence of KB cancer cells and FB cells in 10% human blood plasma. To determine the

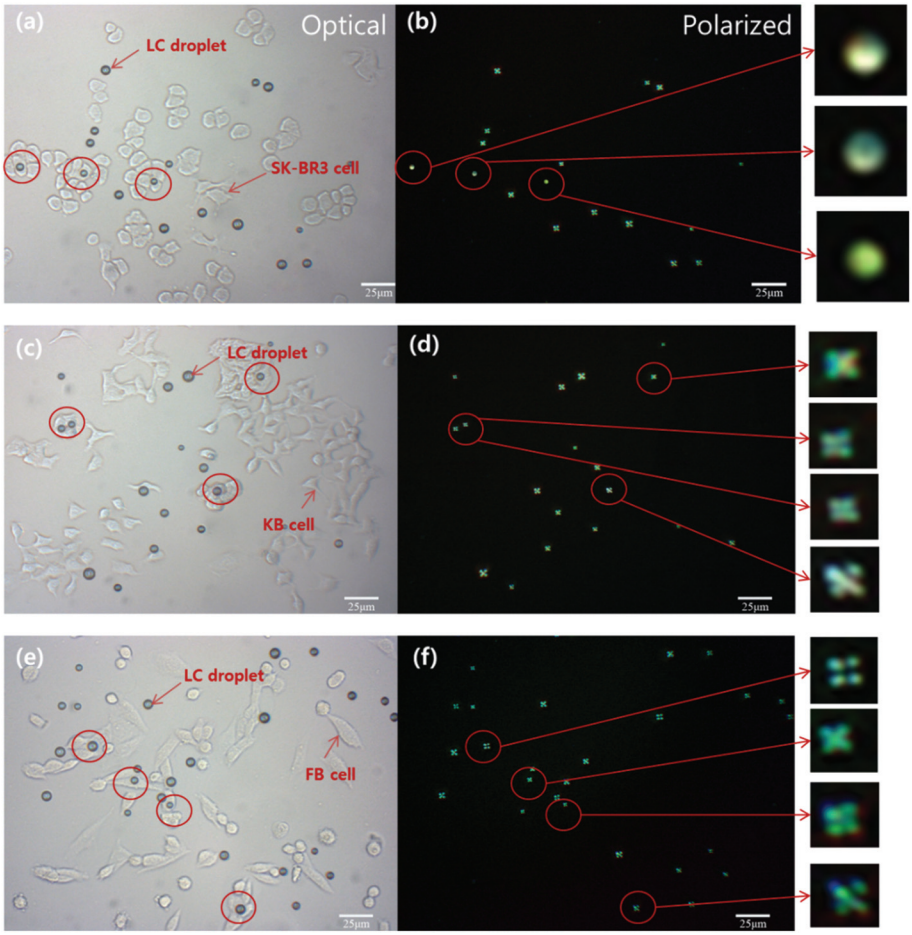

Fig. 6 Optical (left) and polarized light (right) images of herceptin-conjugated LC microdroplets showing interactions with membrane spread SK-BR3 cancer cells (a, b), KB cancer cells (c, d) and FB cells (e, f) in 10% human blood plasma.

selectivity of the herceptin-conjugated LC microdroplets, the SK-BR3 cancer cells at a fixed density of 2000 cells per mL were co-cultured with 1.0 mL of the herceptin-conjugated LC microdroplets emulsion in the presence of KB cancer cells and FB cells at 30 °C for 3 h in 10% human blood plasma. To make a visible distinction between the SK-BR3 cancer cells and KB cancer cells or FB cells, the 10% methylene blue-stained SK-BR3 cancer cells were co-cultured with herceptin-anchored LC microdroplets and their images were recorded. The bright field images of the herceptin-conjugated LC microdroplets co-cultured with methylene blue-stained SK-BR3 cancer cells and unstained controlled cells (KB and FB cells) have confirmed the contact of the herceptin-conjugated LC microdroplets with methylene blue-stained SK-BR3 cancer cells (Fig. 7a). The interactions of the SK-BR3 cancer cells (blue colored) with herceptin-conjugated LC microdroplets (Fig. 7a) were able to induce orientation transitions in the 5 CB molecules from radial to bipolar in the herceptin-conjugated LC microdroplets as confirmed by their polarised light micrograph (Fig. 7b). The orientation transitions from radial to bipolar in the 5CB molecules in the polarised light micrograph of the herceptin-conjugated LC microdroplets are shown by red circles in Fig. 7b, and the same is shown by two lower subsets marked by an arrow in Fig. 7b. These orientation transitions from radial to bipolar in the 5CB molecules upon interactions with the SK-BR3 cancer cells (blue colored) with herceptin-conjugated LC microdroplets have clearly confirmed that herceptin-conjugated LC microdroplets are able to interact selectively with SK-BR3 cancer cells and the interaction forces are sufficiently strong to cause orientation transitions from radial to bipolar in the 5CB molecules (Fig. 7b).

On the other hand, the interacting KB and FB control cells (white colored) with herceptin-conjugated LC microdroplets remained ineffective at inducing any orientation transition in the 5CB molecules in the herceptin-conjugated LC microdroplets as shown by the red circle in the polarised micrograph (Fig. 7b) and also by the red arrow marked top subset in Fig. 7b. These studies clearly indicated that the herceptin-conjugated LC microdroplets interactions remained quite selective and effective for the SK-BR3 cancer cells without any interference from the co-cultured KB cancer cells and FB control cells.

To exclude the effect of methylene blue staining in the detection of the SK-BR3 cancer cells by the herceptin conju-

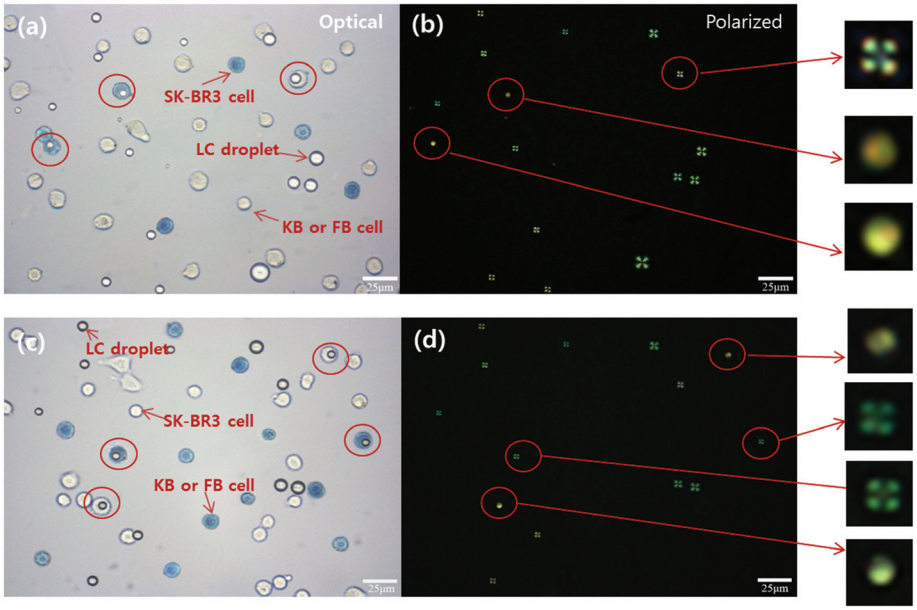

Fig. 7 Optical (left) and polarized light (right) images of herceptin-conjugated LC microdroplets co-cultured with unstained FB cells (white), KB cells (white), and methylene blue stained SK-BR3 cells (blue) (a, b); and herceptin-conjugated LC microdroplets co-cultured with stained FB cells (blue), KB cells (blue), and unstained SK-BR3 cells (white) (c, d) in 10% human blood plasma.

gated LC microdroplets, another set of experiments was also performed by co-culturing the methylene blue stained control cells (KB and FB) and unstained SK-BR3 cancer cells with herceptin-conjugated LC microdroplets at 30 °C for 3 h in 10% human blood plasma, and optical and polarised light micrographs were recorded (Fig. 7c and d) to confirm the contact of the cells and orientation state of the 5CB molecules in the herceptin-conjugated LC microdroplets. The red circled interactions (Fig. 7c) of the herceptin-conjugated LC microdroplets with SK-BR3 cancer cells (white colored) were able to induce an orientation transition in the 5CB molecules from radial to bipolar, as shown by circles in the polarised light micrograph (Fig. 7d) and by the red arrow marked top and bottom subsets in Fig. 7d. On the other hand, the red circled interactions (Fig. 7c) of the herceptin-conjugated LC microdroplets with the KB cancer cells and FB cells (blue colored) remained ineffective at inducing any orientation transition in the 5CB molecules in the herceptin-conjugated LC microdroplets, as shown by the red circles in the polarised light micrograph (Fig. 7d) and by the red arrow marked two middle subsets in Fig. 7d. These results clearly indicated that the selectivity of the herceptin-conjugated LC microdroplets remained unchanged upon staining the SK-BR3 cancer cells with methylene blue, and the selectivity of the herceptin-conjugated LC microdroplets remained unaltered in the presence of KB cancer cells, FB normal cells and 10% blood plasma. The selectivity of the herceptin-conjugated LC microdroplets for the detection of SK-BR3 cancer cells is comparable to an aptamer based electrochemical biosensor[66] used for the detection of SK-BR3 cancer cells in the presence of other control cancer cells such as human prostate cells, HER2 poorly expressed breast cancer cells, and colon tumors cells.

4. Conclusions

A SK-BR3 human breast cancer cell selective biosensor has been developed using the herceptin-conjugated LC microdroplets emulsion. The optical properties of the 5CB molecules were utilized to develop cell selective signals based on antibody–antigen interactions.[57,68] The SDS surfactant played a significant role in controlling the orientation of the 5CB molecules in the LC microdroplets[66,67] and herceptin-conjugated PS-*b*-PA block copolymer also added SK-BR3 cancer cells selectivity as it acted as a sensitive transducer for transmitting the interfacial interaction forces to the core of the LC microdroplets to develop naked eye detectable signals *via* an orientation transition in the 5CB molecules. These studies also confirmed that herceptin is able to interact effectively and selectively with the HER2+ biomarker expressed on SK-BR3 human breast cancer cells without any interference from other control cells such as KB cancer cells, FB normal cells and without interference from blood plasma proteins. The antibody anchored LC microdroplets emulsion approach is potentially useful for the development of a label free optical biosensor for *in vitro* detection of SK-BR3 human breast cancer cells in biological fluids without wasting time on sample preparation. Further work is in progress to develop LC microdroplets based biosensors for the detection of other cancer cells and biomolecules using functional polymers and surfactants with different properties.

Conflict of interest

The authors declare no competing financial interest.

Authors contributions

Ms Wang Ding is a student of master of engineering at Department of Polymer Science and Engineering at Kyungpook National University Daegu, South Korea and made substantial contribution in designing the experiment and acquisition of the data. Prof. Soo-Young Park and Prof. Young-Kyoo Kim helped in analysis of data. Prof. Kailash Chandra Gupta has participated in critical discussion on the contents and drafting the manuscript for publication. Prof. Inn-Kyu Kang has finally given approval after evaluating the contents and discussion.

Acknowledgements

This work was supported by the Basic Research Laboratory Program (No. 2011-0020264) and General Research Program (2013 R1A1A 2005148) from the Ministry of Education, Science and Technology of Korea. One of the authors, Prof. K. C. Gupta, is thankful to Prof. Inn-Kyu Kang for sponsoring his visit to Department of Polymer Science and Engineering as Visiting Professor for collaborative research.

References

1 V. J. Alino, J. Pang and K. L. Yang, *Langmuir*, 2011, **27**, 11784.
2 X. Ding and K.-L. Yang, *Sens. Actuators, B*, 2012, **173**, 607.
3 S. Sivakumar, K. L. Wark, J. K. Gupta, N. L. Abbott and F. Caruso, *Adv. Funct. Mater.*, 2009, **19**, 2260.
4 M. Khan and S. Y. Park, *Sens. Actuators, B*, 2014, **202**, 516.
5 S. He, W. Liang, C. Tanner, K.-L. Cheng, J. Fang and S.-T. Wu, *Anal. Methods*, 2013, **5**, 4126.
6 J. M. Brake, M. K. Daschner, Y.-Y. Luk and N. L. Abbott, *Science*, 2003, **302**, 2094.
7 X. Bi, D. Hartono and K. L. Yang, *Adv. Funct. Mater.*, 2009, **19**, 3760.
8 Q.-Z. Hu and C.-H. Jang, *Bull. Korean Chem. Soc.*, 2011, **32**, 4377.
9 M. Khan and S. Y. Park, *Colloids Surf., B*, 2015, **127**, 241.
10 J.-M. Seo, W. Khan and S.-Y. Park, *Soft Matter*, 2011, **8**, 198.
11 V. J. Aliño, P. H. Sim, W. T. Choy, A. Fraser and K.-L. Yang, *Langmuir*, 2012, **28**, 17571.
12 L. N. Tan, V. J. Orler and N. L. Abbott, *Langmuir*, 2012, **28**, 6364.
13 X. Ding and K.-L. Yang, *Anal. Chem.*, 2013, **85**, 10710.
14 Q. Z. Hu and C. H. Jang, *J. Biotechnol.*, 2012, **157**, 223.
15 S. Yang, C. Wu, H. Tan, Y. Wu, S. Liao, Z. Wu, G. Shen and R. Yu, *Anal. Chem.*, 2013, **85**, 14.
16 C. H. Chen and K. L. Yang, *Anal. Biochem.*, 2012, **421**, 321.
17 Q. Zhu and K.-L. Yang, *Anal. Chim. Acta*, 2015, **853**, 696.
18 A. D. Price and D. K. Schwartz, *J. Am. Chem. Soc.*, 2008, **130**, 8188.
19 S. Yang, Y. Liu, H. Tan, C. Wu, Z. Wu, G. Shen and R. Yu, *Chem. Commun.*, 2012, **48**, 2861.
20 S. L. Lai, S. Huang, X. Bi and K.-L. Yang, *Langmuir*, 2008, **25**, 311.
21 J. G. Reeder and V. G. Vogel, *Breast cancer prevention. Advances in Breast Cancer Management*, Springer, 2nd edn, 2008, p. 149.
22 B. Lerner, *Pink Ribbon Fatigue*, Times, New York, 2010, p. 11.
23 P. C. Gøtzsche and K. J. Jørgensen, *Screening for breast cancer with mammography*, The Cochrane Library, 2013.
24 H. D. Nelson, K. Tyne, A. Naik, C. Bougatsos, B. K. Chan and L. Humphrey, *Ann. Intern. Med.*, 2009, **151**, 727.
25 C. E. DeSantis, C. C. Lin, A. B. Mariotto, R. L. Siegel, K. D. Stein, J. L. Kramer, R. Alteri, A. A. S. Robbins and A. Jemal, *CA-Cancer J. Clin.*, 2014, **64**, 252.
26 M. J. van de Vijver, Y. D. He, L. J. van 't Veer, H. Dai, A. A. M. Hart, D. W. Voskuil, G. J. Schreiber, J. L. Peterse, C. Roberts, M. J. Marton, M. Parrish, D. Atsma, A. Witteveen, A. Glas, L. Delahaye, T. van der Velde, H. Bartelink, S. Rodenhuis, E. T. Rutgers, S. H. Friend and R. Bernards, *N. Engl. J. Med.*, 2002, **347**, 1999.
27 S. Shak, *Seminars in oncology*, 1999, p. 71.
28 C. Vogel, M. Cobleigh, D. Tripathy, J. Gutheil, L. Harris, L. Fehrenbacher, D. J. Slamon, M. Murphy, W. F. Novotny, M. Burchmore, S. Shak and S. J. Stewart, *Eur. J. Cancer*, 2001, **37**, 25.
29 T. M. Suter, M. Procter, D. J. van Veldhuisen, M. Muscholl, J. Bergh, C. Carlomagno, T. Parren, R. Passalacqua, C. Bighin, J. G. Klijn, F. T. Agreev, E. T. Hitre, J. Groetz, H. Iwata, M. Knap, M. Gnant, S. Muehlbauer, A. Spencse, R. D. Gelbert and M. J. Piccart, *J. Clin. Oncol.*, 2007, **25**, 3859.
30 M. Procter, T. M. Suter, E. de Azambuja, U. Dafni, V. Dooren, S. Muehlbauer, M. A. Climent, E. Rechberger, W. T.-W. Liu, M. Toi, R. C. Coombes, D. Dodwell, O. Pagani, J. Madrid, M. Hall, S.-C. Chen, C. Focan, M. Muschol, D. J. van Veldhuisen and M. J. Piccart-Gebhart, *J. Clin. Oncol.*, 2010, **28**, 3422.
31 E. H. Romond, E. A. Perez, J. Bryant, V. J. Suman, C. E. Geyer, N. E. Davidson, E. Tan-Chiu, S. Martino, S. Paik, P. A. Kaufman, S. M. Swain, T. M. Pisansky, L. Fehrenbacher, L. A. Kutteh, V. G. Vogel, D. W. Visscher, G. Yothers, R. B. Jenkins, A. M. Brown, S. R. Dakhil, E. P. Mamounas, W. L. Lingle, P. M. Klein, J. N. Ingle and N. Wolmark, *N. Engl. J. Med.*, 2005, **353**, 1673.
32 S. Suleman, *Semin. Nucl. Med.*, 2013, **43**, 271.
33 C. H. Kao, S. J. Wang and S. H. Yeh, *Clin. Nucl. Med.*, 1994, **19**, 898.
34 R. L. Wahl, R. L. Cody, G. D. Hutchins and E. E. Mudgett, *Radiology*, 1991, **179**, 765.
35 L. P. Adler, J. P. Crowe, N. K. Al-Kaisi and J. L. Sunshine, *Radiology*, 1993, **187**, 743.

36 T. B. Evers, in *Breast Cancer*, ed. K. K. Hunt, G. L. Robb, E. A. Strom and N. T. Ueno, Springer, New York, 2nd edn, 2008, p. 27.
37 H. Palmedo, H. J. Biersack and S. Lastoria, *Eur. J. Nucl. Med.*, 1998, **25**, 375.
38 I. Khalkhali, J. Villanueva-Meyer and S. L. Edell, *J. Nucl. Med.*, 2000, **41**, 1973.
39 D. J. Samson, C. R. Flamm, E. D. Pisano and N. Aronson, *Acad. Radiol.*, 2002, **9**, 773.
40 N. Houssami, R. Turner and M. Morrow, *Ann. Surg.*, 2013, **257**, 249.
41 N. Houssami, R. Turner, P. Macaskill, L. W. Turnbull, D. R. McCready, T. M. Tuttle, N. Wapiwala and L. J. Solin, *J. Clin. Oncol.*, 2013, **52**, 7515.
42 F. Shamsipour, A. H. Zarnani, R. Ghods, M. Chamankhah, F. Forouzesh, S. Vafaei, A. A. Bayat, M. M. Akhondi, M. A. Oghabian and M. Jeddi-Tehrani, *Avicenna J. Med. Biotechnol.*, 2009, **1**, 27.
43 M. A. Oghabian1, M. Jeddi-Tehrani, A. Zolfaghari, F. Shamsipour, S. Khoei and S. Amanpour, *J. Nanosci. Nanotechnol.*, 2011, **11**, 5340.
44 I. Hilger, R. Trost, J. R. Reichenbach, W. Linb, M. R. Lisy, A. Berndt and W. A. Kaiser, *Nanotechnology*, 2007, **18**, 1.
45 S. Jiang, Y. Zhang, K. M. Lim, E. K. Sim and L. Ye, *Nanotechnology*, 2009, **20**, 155101.
46 M. Rimmele, *ChemBioChem*, 2003, **4**, 963.
47 K. Zhang, K. Sefah, L. Tang, Z. Zhao, G. Zhu, M. Ye, W. Sun, S. Goodison and W. Tan, *ChemMedChem*, 2012, **7**, 79.
48 G. H. Heppner and S. R. Wolman, *Breast J.*, 1999, **5**, 122.
49 P. J. Dawson, S. R. Wolman, L. Tait, G. H. Heppner and F. R. Miller, *Am. J. Pathol.*, 1996, **148**, 313.
50 A. R. Wise, J. A. Nye and J. T. Groves, *ChemPhysChem*, 2008, **9**, 1688.
51 D. Hartono, X. Y. Bi, K. L. Yang and L. Y. L. Yung, *Adv. Funct. Mater.*, 2008, **18**, 2938.
52 T. Bera and J. Y. Fang, *Langmuir*, 2013, **29**, 387.
53 D. Hartono, C. Y. Xue, K. L. Yang and L. Y. L. Yung, *Adv. Funct. Mater.*, 2009, **19**, 3574.
54 F. Zuo, Z. Liao, C. Zhao, Z. Qin, X. Li, C. Zhang and D. Liu, *Chem. Commun.*, 2014, **50**, 1857.
55 M. L. Bungabong, P. B. Ong and K. L. Yang, *Sens. Actuators, B*, 2010, **148**, 420.
56 H. J. VanTreeck, D. R. Most, B. A. Grinwald, K. A. Kupcho, A. Sen, M. D. Bond and B. R. Acharaya, *Sens. Actuators, B*, 2011, **158**, 104.
57 K. Lee, K. C. Gupta, S. Y. Park and I.-K. Kang, *J. Mater. Chem. B*, 2016, **4**, 704.
58 C.-Y. Xue and K.-L. Yang, *Langmuir*, 2008, **24**, 563.
59 C.-S. Xue, S. A. Khan and K.-L. Yang, *Adv. Funct. Mater.*, 2008, **21**, 198.
60 R. Ondris-Crawford, E. P. Boyko, B. G. Wagner, J. H. Erdmann, S. Žumer and J. W. Doane, *J. Appl. Phys.*, 1991, **69**, 6380.
61 N. A. Lockwood and N. L. Abbott, *Curr. Opin. Colloid Interface Sci.*, 2005, **10**, 111.
62 J. M. Brake and N. L. Abbott, *Langmuir*, 2002, **18**, 6101.
63 Y. Choi, K. Lee, K. C. Gupta, S. Y. Park and I.-K. Kang, *J. Mater. Chem. B*, 2015, **3**, 8659.
64 J.-H. Lee, T. Kamal, S. V. Roth, P. Zhang and S.-Y. Park, *RSC Adv.*, 2014, **4**, 40617.
65 M. A. Gharbi, M. Nobili and C. Blanc, *J. Colloid Interface Sci.*, 2014, **417**, 250.
66 F. Liu, Y. Zhang, J. Yu, S. Wang, S. Ge and X. Song, *Biosens. Bioelectron.*, 2014, **51**, 413.
67 A. F. Nieves, G. Cristobal, V. G. Chavez, G. C. Spalding, K. Dholakia and D. A. Weitz, *Adv. Mater.*, 2005, **17**, 680.
68 S. H. Yoon, K. C. Gupta, J. S. Borah, S. Y. Park, Y. K. Kim, J. H. Lee and I.-K. Kang, *Langmuir*, 2014, **30**, 10668.

